A Comparison between Stepwise Modelling and Inverse Modelling Methods for Characterization of Press Hardened Sheet Metals.

Stefan Marth [1], Hans-Åke Häggblad [1] and Mats Oldenburg [1]

Abstract

The demand for weight reduction of cars has increased the number of press hardened sheet metal parts used in the automotive industry. This leads to an increased demand on the precision of simulations of press hardened sheet metals. An accurate prediction of the post-necking behaviour of materials is therefore needed to increase the precision of computer simulations with large deformations, as for example in forming simulations and crash simulations. Especially fracture simulations of press hardened steel parts with tailored properties have a huge demand on precise material models.

Inverse modelling is a common engineering tool to characterize the elasto-plastic behaviour of materials. Taking experimental data, such as force and displacement data, the material model parameters are optimised until the simulated output reaches a target function. Then inverse modelling is highly time demanding and needs nonlinear hardening material models.

Lately a new fast method for post necking characterisation of sheet metals, called the Stepwise Modelling Method (SMM), was presented. This method uses full field measurements to obtain the strain field on the surface of sheet metal tensile specimens. Furthermore, the stepwise modelling method models an experimental hardening curve in a stepwise process. This hardening curve is a piecewise linear curve and not restricted to any specific material model.

In this paper SMM is used to characterize the hardening behaviour for thermally treated boron steel. These results are compared with the results of inverse modelling. Three different material models are used. The comparison shows a minor deviation in the resulting hardening relations between stepwise modelling and inverse modelling. Since the efficiency is an important factor in product development calculation times are taken into account. Comparing calculation time using SMM is considerably more efficient than using inverse modelling. Furthermore another advantage of SMM is shown in the fact that the piecewise linear hardening curves can be fitted to almost any material model without computational costs.

1 Introduction

The amount of ultra-high strength steel (UHSS) in car structures is constantly increasing. The main driving force is weight reduction while maintaining crash safety. The material modelling

requires precise material characterisation methods to ensure reliable results. A common method to characterise material models is the inverse modelling described by Tarantola [1]. In inverse modelling a problem is parameterised and by varying parameters an object function is optimized. Recently Marth et al. [2] presented the Stepwise Modelling Method (SMM), a method that is able to characterize post necking hardening behaviour of material deformed under plane stress condition. This method optimizes the calculated force value with the experimentally obtained forces for each time step by varying the hardening parameter of a stepwise linear hardening relation.

In this paper the SMM is applied to determine the stepwise linear hardening relation for a ferritic boron steel. This result is used to characterize three different material models; the Voce, Swift and El-Magd material model. As a comparison an inverse modelling for each material model based on finite element analysis is performed. The obtained parameters for these material models are presented. For comparison these parameters are used in finite element simulations of a tensile test. As a measure of efficiency the calculation times for both the stepwise modelling method and the inverse modelling method are presented and compared.

2 Methods and Material

The characterization of the post necking hardening of boron steel is performed by using two different methods which will be described in this section; the Inverse Modelling and the Stepwise Modelling methods. The material chosen for this study is based on the boron steel USIBOR 1500 produced by ArcelorMittal. The microstructure composition was changed by heating to austenitization temperature and cooled by a controlled cooling rate. The finale microstructure composition was characterized by Östlund et al. [3] and has a ferritic microstructure.

2.1 Experiment

A sheet metal tensile test with notched 1.2 mm thick specimen with dimensions as shown in Figure 1 is performed. The test is performed as quasi static tensile test. During testing the force, elongation over a 50 mm gauge length and the deformation field on the specimen's surface are measured. The deformation measurement on the surface is performed by the Digital Image Correlation (DIC) using the commercial software ARAMIS, delivered by GOMmbH. During each test a series of 50-100 images are taken.

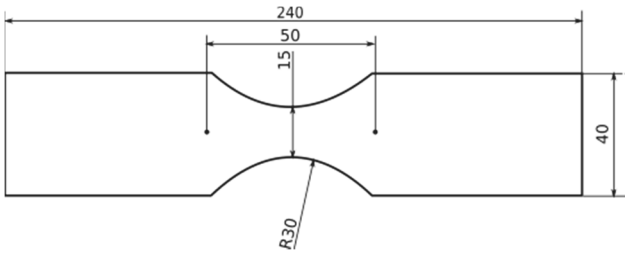

Figure 1: *Notched tensile specimen; Sheet thickness: 1.2mm; Gauge length: 50mm*

2.2 Stepwise Modelling Method

To stepwise model the post necking hardening behaviour of sheet metals was recently presented by Marth et al. [2]. The SMM is based on digital speckle photography (DSP), taken from the previous described experiment and results in a piecewise linear hardening relation. Based on the observed deformation field the plane strain field is calculated and by assuming incompressibility the resulting through thickness strains are determined. By assuming isotropic von Mises plasticity the stress tensor can be calculated based on the derived strain tensor using a radial return algorithm. To characterize the hardening behaviour the stress strain relation is modelled step by step for each image taken during the experiment. For each step the residual between the resulting force through an integration path across the specimen's cross section and the experimentally measured force are minimized by adapting the current linear hardening coefficient. The characterisation of material model parameters is performed using a least square fit to the piecewise linear hardening curve, obtained by SMM. By using this method almost any elasto-plastic material model can be characterised in a simple manner.

2.3 Inverse Modelling Method

The inverse modelling is performed by using the software LS-OPT for the optimisation and LS-DYNA as solver for the finite element method (FEM) calculations. The different material models are presented in the following section. For each material model three or four parameters are optimised. The lower and upper bounds for each parameter are presented in Table 1. The start value for each parameter is chosen as the middle value between the bounds. During the optimization a Mean Squared Error (MSE) for the discrepancy between the experimental obtained force-elongation and the FEM simulation force-elongation, is minimized. The optimisation uses a leap-frog optimizer (LFOP) algorithm as suggested in the LS-OPT manual [4]. The explicit FEM simulation uses 4 node shell elements with an average side length of 0.2mm modelling the 50mm length of the notched tensile specimen. The FEM model is composed of 45.343 fully integrated quadratic Belytschko-Tsay shell elements.

Table 1: *Input data for inverse modelling. Lower and upper bounds of material parameters*

Material model	**Bounds**	**Parameters**			
		C_1	**C_2**	**C_3**	**C_4**
Swift	Lower	900 [MPa]	$1 \cdot 10^{-3}$ [-]	0.1[-]	-
	Upper	1000 [MPa]	$5 \cdot 10^{-3}$ [-]	0.5[-]	-
Voce	Lower	750 [MPa]	400 [MPa]	5 [-]	-
	Upper	850 [MPa]	500 [MPa]	15 [-]	-
El-Magd	Lower	400 [MPa]	300 [MPa]	200 [MPa]	10 [-]
	Upper	500 [MPa]	400 [MPa]	300 [MPa]	30 [-]

2.4 Material Models

The inverse modelling and the stepwise modelling methods are used to calibrate three different material models, which will be briefly presented in this section. All models are not temperature or strain rate dependent and are a pure functions of the effective plastic strain, $\bar{\varepsilon}^p$. The mathematical equation of the Swift model [5] is presented in Equation 1, where C_1 to C_3 are constant material parameter.

$$\sigma(\bar{\varepsilon}^p) = C_1 \cdot \left(C_2 + \bar{\varepsilon}^p\right)^{C_3} \tag{1}$$

The mathematical equation of the Voce model [6] is presented in Equation 2, where C_1 to C_3 are constant material parameter.

$$\sigma(\bar{\varepsilon}^p) = C_1 + (C_2 - C_1) \cdot \exp\left(-C_3 \cdot \bar{\varepsilon}^p\right) \tag{2}$$

The mathematical equation of the El-Magd model [7] is presented in Equation 3, where C_1 to C_4 are constant material parameter.

$$\sigma(\bar{\varepsilon}^p) = C_1 + (C_2 \cdot \bar{\varepsilon}^p) + C_3 \cdot \left[1 - \exp\left(-C_4 \cdot \bar{\varepsilon}^p\right)\right] \tag{3}$$

While the Voce material model has a maximum stress value, C_1, both the Swift and the El-Magd model are constantly increasing the stress with increasing strains. The El-Magd model can be seen as an extended Voce model with the constant linear factor, C_2.

3 Results and Discussion

Characterizations of the boron steel for the described material models are performed using SMM and inverse modelling. The characterization of these different material models based on SMM is validated by comparing FEM simulations with the experimental results.

3.1 Characterization

The resulting piecewise linear hardening behaviour of the material using SMM is presented in Figure 2 as a solid line. This SMM curve has a maximum effective plastic strain of 0.74, which is the locally measured fracture strain, marked with a cross. The resulting hardening relations for the three presented material models based on the inverse modelling method are added to Figure 2 as dashed lines. The resulting stress-strain relation obtained by SMM is a piecewise linear curve and has therefore not the smooth shape of the material models. However, the Swift (dotted line) and El-Magd (dash-dot line) material models show an overall similar result as the presented SMM result. Only the Voce (dashed line) model does not fit to these results, especially for effective plastic strains higher than 0.3. This is mainly based on constrains of this material model, which represents ideal plastic materials better for high strain values.

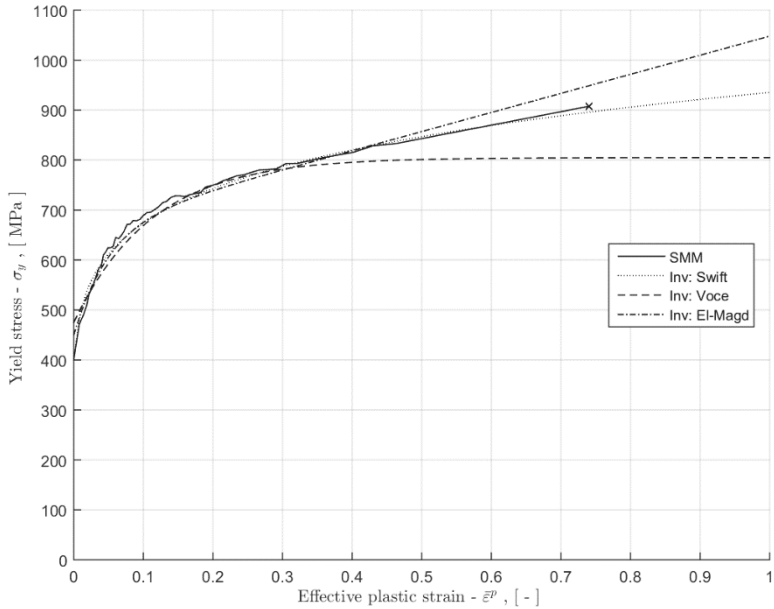

Figure 2: *Resulting stress-strain relation from SMM and Inverse modelling*

Using a simple curve fitting based on the piecewise linear hardening curve obtained by SMM the parameters for the three material models can be found and compared with the parameters from inverse modelling. Table 2 shows the summary of the different parameters obtained from the SMM and inverse modelling method. It can be seen that both methods based on the same experiment result in similar parameters. The smallest difference can be seen for the Swift material model, where the deviations between the parameters are nearly negligible. Comparing the piecewise linear curve and the Swift curve in Figure 2 a similar behaviour can be seen. The largest deviation is obtained for the Voce material model.

Table 2: *Resulting parameters from SMM and inverse modelling*

Material model	Method	Parameters			
		C_1	C_2	C_3	C_4
Swift	SMM	947 [MPa]	$2.16 \cdot 10^{-3}$ [-]	0.146 [-]	-
	Inverse	935 [MPa]	$2.81 \cdot 10^{-3}$ [-]	0.144 [-]	-
Voce	SMM	813 [MPa]	458 [MPa]	10.3 [-]	-
	Inverse	805 [MPa]	475 [MPa]	8.87 [-]	-
El-Magd	SMM	411 [MPa]	308 [MPa]	280 [MPa]	22.9 [-]
	Inverse	450 [MPa]	382 [MPa]	216 [MPa]	20.2 [-]

In Table 3 a compilation of the computation time needed for both SMM and inverse modelling is shown. The time measured the amount of computational calculation time required on a stationary personal computer under similar conditions. As a comparison between both methods, a relative time factor is presented. For SMM the computing time is approximately the same for all presented material models. Even though only the computational calculation time is presented and the time for experimental setups are not included, is the computational calculation time demand one of the main factors when comparing the efficiency of the methods.

Table 3: *Computation calculation time for SMM and inverse modelling*

	SMM	Inverse modelling		
		Swift	Voce	El-Magd
Computing time [s]	78	21 864	28 584	23 560
Approx. time factor to SMM	-	280	370	300

3.2 Validation

For validating the material parameters obtained by SMM, FEM simulations are performed using the same finite element model as for the inverse modelling. In total four simulations are performed using the stepwise linear, Swift, Voce and El-Magd material model. In inverse modelling the force elongation relation is used as input data for the object function. However, for SMM the force elongation data is not used as input data and therefore it is possible to use it for validation of the material model characterization. The comparison of the force-elongation relation from these validation simulations with the experimental measured values, are shown in Figure 3. The resulted force-elongation relations for all material models are comparable with the experimental obtained relation. Using the piecewise linear hardening model gives a response which is close to the experimental values. The model with the largest deviation is the Voce model (dashed line), which deviates the most at the end of the simulation. The largest deviation of the Swift model (dotted line) can also be found at the end of the simulation; otherwise it follows the experimental curve well. The El-Magd model (dash-dot line) follows largely the experimental curve.

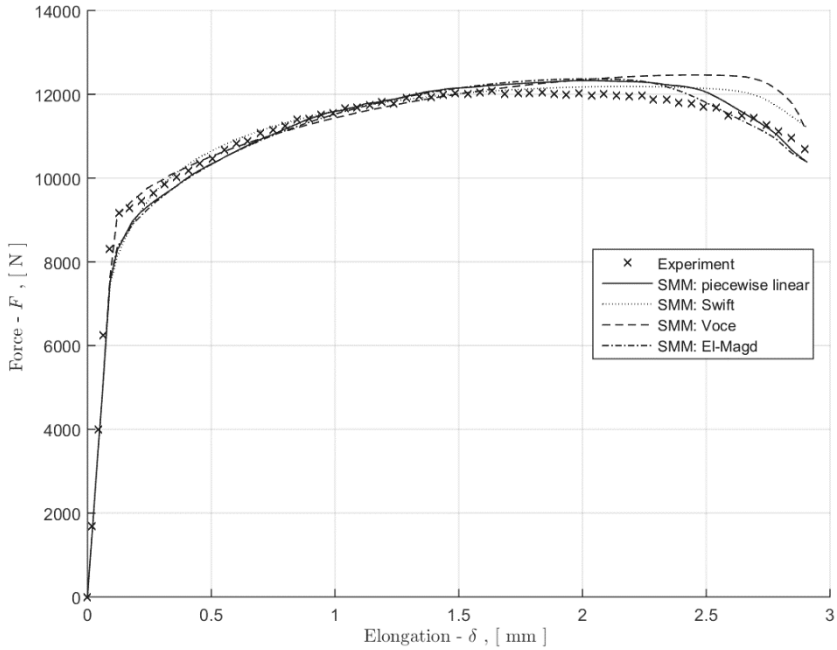

Figure 3: *Comparison of the force-elongation relations from the experiment with FEM simulations based on SMM material-models*

To provide a measure of the discrepancy between simulation results and experimental data a mean squared error, e, is used.

$$e = \frac{1}{P}\sum_{i=1}^{P}\left[\frac{f_i - F_i}{F_{\max}}\right]^2 \tag{4}$$

Where P is the number of measured force-elongation pairs and F_i are the measured force and f_i the corresponding components of the simulated force f. To obtain a dimensionless error the values are normalized using the maximum value of the target curve $F_{max} = \max |F_i|$. Here is $F_{max} = 12.08$ kN and P=62.

The mean squared error, according to Equation 4, obtained for the force-elongation relations based on the SMM results is summarized in Table 4. The MSE for the simulation, using the piecewise linear hardening model, has the smallest error. The inverse modelling method uses the same definition of the MSE (Equation 4) to minimize the deviation between the experimental result and the simulated force-elongation relation, where the design parameter is set to: $e \leq 1 \cdot 10^{-3}$. It is shown

that the MSE for nearly all simulations is smaller than the design parameter used in the inverse modelling. Only the error for the simulation using the Voce material model has a larger value, see Table 4.

Table 4: *Mean squared error, e, of the deviation between the experimental and the simulated force-elongation relation based on the SMM results*

Piecewise linear	Swift	Voce	El-Magd
$6.68 \cdot 10^{-4}$	$8.35 \cdot 10^{-4}$	$1.36 \cdot 10^{-3}$	$6.76 \cdot 10^{-4}$

4 Conclusions

In this paper the results from post necking characterisations using stepwise modelling method and inverse modelling method are compared. It is concluded that both methods are characterising the post necking behaviour in a reliable and accurate way. The piecewise linear result of the SMM gives a higher flexibility since it is not coupled to any specific material model and can quickly and easily be adapted to any material model. The SMM is considerably faster than the inverse modelling method. Simulations using the different material models characterized by SMM show accurate responses in the force elongation relation compared with experimental measures. Finally it can be stated that the Voce material model is not a good choice for modelling the post necking behaviour of boron steel with a ferritic microstructure when very large strains occur.

References

[1] Tarantola, A. Inverse problem theory: methods for data fitting and model parameter estimation. Amsterdam: Elsevier; 1987.

[2] Marth, S. et al. Post necking characterisation for sheet metal materials using full field measurement, Journal of Materials Processing Technology (2016), 238, pp. 315-324.

[3] Östlund R. et al. Evaluation of localization and failure of boron alloyed steels with different microstructure compositions, Journal of Materials Processing Technology (2014), 214, pp. 592-598.

[4] Stander, N. et al. LS-OPT User's Manual. Livermore Software Technology Corporation, California (2014).

[5] Swift, H., Plastic instability under plane stress, Journal of the Mechanics and Physics of Solids (1952), 1, pp. 1-18.

[6] Voce, E., The relationship between stress and strain for homogeneous deformations. Journal of the Institute of Metals (1948), 74, pp. 537-562.

[7] K. Stiebler et al., Description of the flow behaviour of a high strength austenitic steel under biaxial loading by a constitutive equation, Nuclear Engineering and Design (1991), 127, pp. 85-93.

Affiliation

[1] Luleå University of Technology, Division of Mechanics of Solid Materials, Luleå, Sweden, stefan.marth@ltu.se